APPLICATION OF DYNAMIC PROBABILISTIC RISK ASSESSMENT TO A SEISMICALLY-INDUCED INTERNAL FLOOD EVENT

Z. Jankovsky[1], R. Denning[2], T. Aldemir[1], H. Sezen[1], J. Hur[1]

[1] *The Ohio State University, Columbus, Ohio, USA, 43210*
[2] *2041 Hythe Rd, Columbus, Ohio, USA, 43220, denningrs.8@gmail.com*

A dynamic event tree analysis (DET) approach is taken to analyze a scenario involving seismically-induced failure of feed-water lines exiting two redundant condensate storage tanks. A fast running, reduced order room flooding model is used to assess the time-dependent flooding of rooms containing critical safety equipment. Time-dependent, probabilistic recovery models are developed for the recovery of auxiliary feed-water flow using FLEX equipment (a portable pumping system), high pressure injection flow, and operability of primary system pilot operated relief valves. A time-dependent, probabilistic aftershock model is applied to determine the effect of aftershocks on the timing of recovery actions. An ADAPT (dynamic event tree) approach to DET analysis is used in which branching occurs for a MELCOR (severe accident analysis code) model of transient system behavior leading up to the point of core damage or no core damage for a spectrum of scenarios. The potential value of DET methods in addressing scenarios involving complex timing issues is illustrated.

I. INTRODUCTION

Using techniques being developed within the Light Water Reactor Sustainability Program of the U.S. Department of Energy for analyzing multi-physics problems and performing uncertainty analyses, The Ohio State University is developing a set of computational tools referred to as the DINOSAUR package[1], for integrating the external and internal event elements of a seismic probabilistic risk assessment (SPRA). The DINOSAUR tools are being developed on the MOOSE[2] computational platform and employing the RAVEN[3] code to manage uncertainty analyses. An important characteristic of seismic events is the potential for common cause failure (CCF) of safety related equipment. These common cause relationships can arise as the result of the transmittal of loads to equipment through common structures or as the result of seismically-induced secondary hazards such as seismically-induced floods or seismically-induced fires. Another characteristic of seismic events is the dynamic nature of the events themselves, including the potential for aftershocks, either leading to additional damage to equipment or to the disruption of recovery actions. Within this research program, case studies are being used to support the development and testing of the tools. The case study described in this paper addresses both CCF and the dynamic behavior of the event. A seismic event that not only leads to the failure of some safety related equipment but also to equipment failures resulting from the flooding of equipment following failure of a condensate storage tank (CST) is under consideration. The recovery of safety-related equipment, including FLEX equipment[4], potentially leads to the prevention of core damage depending on how quickly recovery occurs. The impact of aftershocks in delaying recovery actions is also considered.

A dynamic event tree (DET) approach[5] is used for this case study. DETs are similar to traditional event trees except that the branch points are not selected subjectively by the analyst but via the output of a dynamic system model that can describe the evolution of the system in time following the initiating event. The DET approach allows consideration of epistemic and aleatory uncertainties (including operator actions) in a phenomenologically and stochastically consistent framework. In an earlier paper[6] we undertook a quasi-DET approach in which the system transient analysis code, MELCOR[7], was run for a few pre-selected cases. The results of those MELCOR cases were used to develop approximate rules as to the combinations of event timings that would either lead to core damage or prevent core damage. Other aspects of the problem were treated dynamically by performing a large number of time-dependent analyses involving predicted timing of equipment failure and the time required for component recovery. Recovery times were obtained using Monte Carlo sampling from assumed probability distributions for recovery actions. Although the quasi-dynamic analysis provided some important insights that would have been difficult to obtain from a purely static analysis, it was not clear that the rules developed for classifying scenarios as “core damage” or “non-core damage” would have been properly categorized. It was also not possible to de-convolute some aspects of the risk. For

example, in scenarios in which failure of the pilot operated relief valve (PORV) to close resulted in core damage, it was difficult to know whether core damage would have occurred irrespective of PORV behavior.

Section II describes plant design features used in the study. Section III presents the general accident scenario being addressed involving seismically-induced flooding of safety equipment. Sections IV through VIII describe respectively, the component fragility analyses used as a basis for predicting component failure probability as a function of imposed seismic load, the static fault tree/event tree model, the density functions developed to determine the probability of various recovery actions as a function of time, the phenomenological models used, and the ADAPT DET model.[5] Section IX presents the results of the dynamic analyses and Section X presents conclusions.

II. PLANT DESIGN FEATURES

The plant design features for this study do not represent a specific existing plant. The system characteristics are those of a large four-loop pressurized water reactor (PWR). There are two trains of diverse auxiliary feed-water (AFW) systems for which water is supplied from redundant CSTs. A building adjacent to and connected to the auxiliary building by a pipe chase houses the CSTs (see Figure 1). Three high pressure injection (HPI) pumps are located in Basement Room 1 (a single charging pump) and in Basement Room 2 (two HPI pumps which provide high pressure emergency cooling). A fire door separates the two basement rooms. Each room has a drain system, which consists of a small (8 cm diameter) drain in the floor that leads to an assumed semi-infinite sink. The PWR has two primary system pilot operated relief valves (PORVs) which can be operated remotely to reduce the primary system pressure to a level at which adequate flow can be provided to cool the core. The equipment to actuate the PORVs is located in cabinets on the first floor of the auxiliary building. Some operating characteristics of the safety systems are shown as Table I. There are also PORVs on each steam generator.

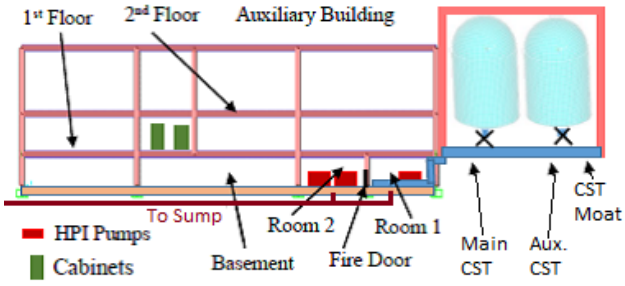

Figure 1 Seismically-Induced Flooding Scenario of HPI Pump Rooms

TABLE I. Safety System Characteristics

Components	Characteristics	Activation Set Point
Pressurizer PORV (2)	Open Set Point Close Set Point	16 MPa 15.5 MPa
HPI (2)	Maximum Pressure Maximum Flow	10 MPa 37.4 kg/s
AFW	Minimum Flow	450 kg/s
Low Pressure Injection (LPI)	Maximum Pressure Maximum Flow	2 MPa 382 kg/s

In the event of loss of feed-water and charging capability, the operators must open the primary system PORVs independently of their automatic set points (see Table I) and implement feed and bleed operations with the HPI safety injection pumps. As a backup to the supply of AFW to the steam generators, FLEX equipment is stored in a protected location on-site. The provision of this FLEX equipment is a post-Fukushima upgrade. This equipment can be transported and connected to a pre-existing interface with the feed-water system. The FLEX equipment uses an alternate source of water, and its use is not precluded by a failure of one or both CSTs.

III. ACCIDENT SCENARIO

The scenario being studied considers a seismic event that leads to failure of one or both of the CSTs. Failure of both CSTs results in the loss of the water source for AFW and the ability to remove heat from the primary system of the PWR. A flow path exists from the CST building to the auxiliary building, as illustrated in Figure 1, such that the basement rooms of the building can be flooded by water in the event of a CST failure. If the water level in a room exceeds 0.67 m in height it is assumed that the pumps in that room will fail to operate. The door between basement Rooms 1 and 2 in Figure 1 is assumed to be hinged to open into Room 2, and would fail when the water level in the Room 1 reaches the 1.67 m level. For this study, it is assumed that loss of the charging pump in Room 1 is unrecoverable. However, when Room 2 dries out, there is a possibility that the HPI function is recoverable. Basement Room 2 is considered dried out when the water level falls below 2.5 cm due to flow through the drain system.

IV. SEISMIC LOADS AND COMPONENT FRAGILITIES

The seismic hazard model for this study is based on an example provided by Ravindra.[8] The core damage frequency is evaluated at three seismic return frequencies 3E-5 yr^{-1}, 1E-5 yr^{-1} and 1E-6 yr^{-1} based on the peak accelerations from the seismic hazard curve. Because the design basis earthquake is established at a return period of 1E-4 yr^{-1} (see Reference 8) and the design requirements for safety related equipment seek a high confidence of a low probability of failure (95 percent confidence of a failure probability less than 0.05), the conditional probability of core damage at the design level is small. As a first step of an SPRA for any plant site a family of seismic hazard curves is developed (each curve representing a vibrational frequency) describing the relationship between peak acceleration at that vibrational frequency and the associated return frequency. The primary vibrational mode of the CSTs is assessed to be approximately 5 Hz. Figure 2 shows the 5 Hz seismic hazard curve describing the relationship between return period and the peak acceleration at this vibrational frequency.

The failure mode of the CST is assumed to be the result of a failure of the bolts fastening the CST to the floor. There are two 20 cm (8 inch) diameter feed-water lines exiting the bottom of each CST. In Figure 1, one of each of the two pipes is indicated at the bottom of the CST with an X describing severance of the line. The load imposed on the piping associated with motion of the tank results in failure of one or more of the lines. Equal probability is assigned to the leak size associated with $0.5A_p$, $1A_p$, $1.5A_p$ and $2A_p$, where $A_p = \pi\ (20/2)^2 = 314.2$ cm^2 is the cross sectional area of a feed-water line. The median acceleration of A_m=1.0g for failure of the CST, log normal standard deviation of β=0.4, and correlation coefficient ρ=0.5 between failure of the two tanks are characteristic values selected for the case study and are not based on analysis. Based on these values, the marginal and joint failure probabilities for the tanks are calculated. Table II shows the 5 Hz accelerations associated with the design basis acceleration and the three return frequencies analyzed. The probability of failure of one of the tanks (Event A) and the probability of failure of both tanks (Event AB) are also shown. The marginal probability of failure of a tank is obtained from the cumulative distribution function of the log normal distribution. The joint failure probability of two tanks was obtained by integrating the probability density function for a bivariate log normal distribution with correlation ρ.

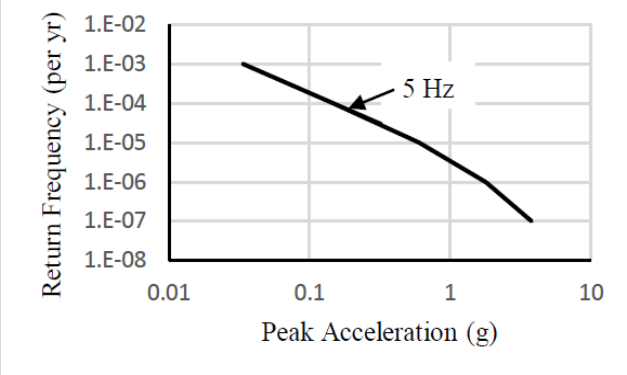

Figure 2. Peak Acceleration versus Return Frequency at Vibrational Frequency of 5 Hz[8]

TABLE II. 5 Hz Spectral Accelerations and Failure Probabilities for CST Failure by Pipe Rupture (A_m=1g, β=0.4, ρ=0.5)

Exceedance Frequency (yr^{-1})	Spectral Acceleration (5 Hz)	Pr (A)	Pr(AB)
1E-4	0.17	4.7E-6	Negligible
3E-5	0.32	2.2E-3	1.6E-4
1E-5	0.6	0.10	3.3E-2
1E-6	1.8	0.93	0.88

Table III provides accelerations and failure probabilities for electrical cabinets (see Figure 1) containing control equipment for the remote operation of the PORVs. Event A refers to the failure of the cabinet for a single PORV, and event AB refers to the loss of cabinets for both PORVs. The loss of a single PORV is assumed to defeat feed and bleed. This is because MELCOR analyses indicate that primary system pressure could not be lowered quickly enough by a single PORV to allow sufficient cooling water injection before core damage occurs. The values for A_m and β are at the low end and high end, respectively, of typical values[8] for equipment, representing potentially vulnerable equipment. In general practice, the value for A_m is based on shaker table tests with a natural frequency of 7.5 Hz and the values for β and ρ are based on expert judgment. The acceleration for the cabinet is multiplied by a factor of 1.5 to account for the higher acceleration experienced on the first floor relative to the ground acceleration, based on the results of a stick model of the auxiliary building[6].

V. FAULT TREE/EVENT TREE MODEL

A generic event tree for a seismically-induced loss of offsite power without recovery is given in Figure 3. Section VI describes the probability distributions that were developed to describe the probability of recovery of failed systems as a function of time. These are summarized in Table IV. It is difficult to analyze recovery actions of this type within the framework of a fixed event tree. When the order of events on the tree can change depending on the progression of the event, a DET approach

is more appropriate.[9] The alternative within a fixed event tree approach is to create multiple entries for each event on a tree. For example, in NUREG-1150 the detailed Level 2 accident progression event trees addressed the potential for hydrogen combustion in the containment at multiple time periods in the accident scenario.[10]

TABLE III. Spectral Accelerations and Failure Probabilities PORV Cabinets (A_m=1g, β=0.6894, ρ=0.5).

Exceedance Frequency (yr^{-1})	**Spectral Acceleration (First Floor)**	**Pr (A)**	**Pr(AB)**
1E-4	0.26	0.025	0.0047
3E-5	0.48	0.14	0.055
1E-5	0.9	0.44	0.28
1E-6	2.7	0.93	0.87

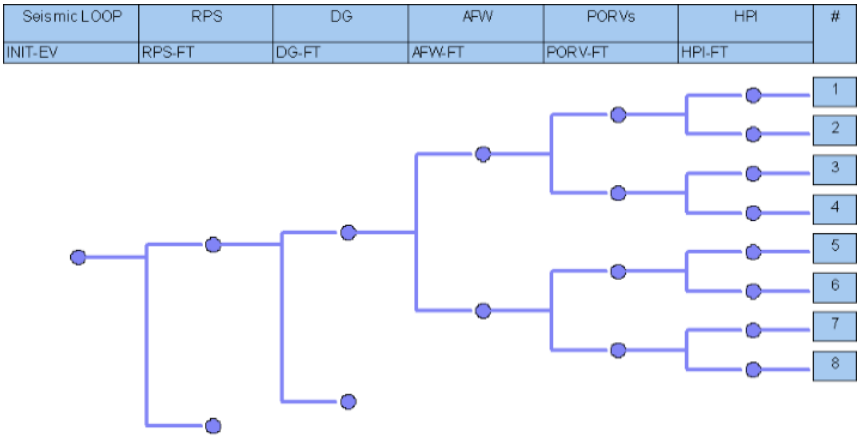

Figure 3. Seismic Event Tree.
(LOOP: loss of offsite power, RPS: reactor protection system, DG: diesel generators, AFW: auxiliary feedwater, PORV: pilot-operated relief valve, HPI: high pressure injection, FT: fault tree).

Fault trees from an internal events PRA provided the framework within which the seismic-induced failures were integrated.[11] The existing front line and support system fault trees were modified to include seismic faults. The seismic-induced failures are included in the fault trees as basic events as shown below for AFW in Figure 4. These "fragility basic events" will then appear in the minimum cutsets and thus indicate which combinations of seismic-induced failures would lead to core damage. Passive components and structures which are not included in non-seismic PRA have been reviewed and additional basic events are added to fault trees. For example, door failure is not normally considered in an internal PRA but in this specific scenario can lead to flood and failure of the two HPI safety injection pumps in Basement Room 2 of the auxiliary building (see Figure 1) and can lead to core damage.

The Level 1 fault tree of the AFW system (Figure 4(a)) was created based on U.S. Nuclear Regulatory Commission's fault tree of AFW system Design Class 2.[11] This fault tree was modified to include the seismically-induced faults as shown in Figure 4(b). The AFW system fault tree top logic is revised to include seismic failure basic events. CST suction failure (basic event) in Figure 4(a) is modified to become the union of random tank failure and seismic-induced CST suction failure in Figure 4(b).

The seismic subtree introduced into the AFW fault tree is shown in Figure 5. CST suction failure is the result of either outlet pipe failure or CST failure given the seismic event. Seismic event is represented as a house event in the model according to U.S. Nuclear Regulatory Commission's (NRC's) External Events Report,[11] to denote a failure that is guaranteed to always occur for the given modeling conditions or is guaranteed to never occur for the given modeling conditions. The seismic subtrees are only activated when the seismic event is quantified and its flag is set to TRUE.

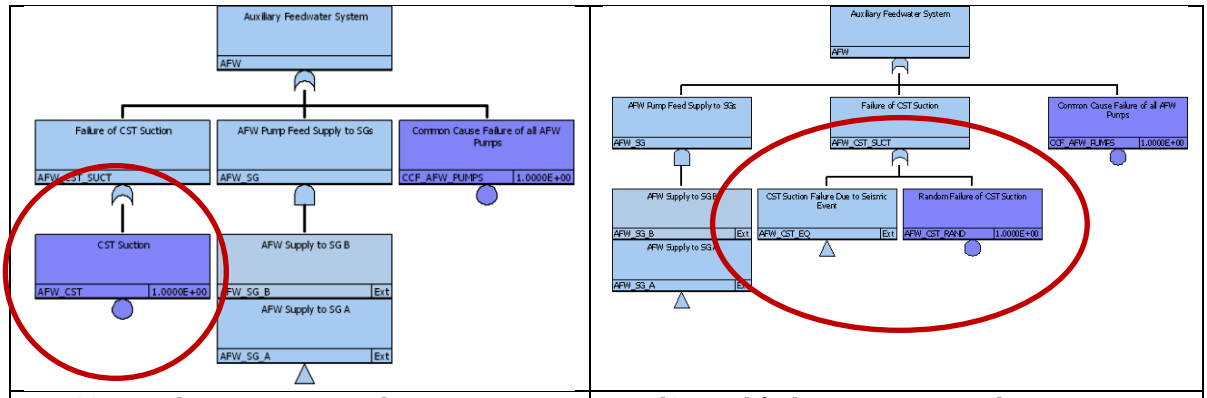

(a) Initial AFW System Fault Tree (b) Modified AFW System Fault Tree

Figure 4. Modification of AFW System Fault Tree to Integrate Seismic Induced Failure

VI. RECOVERY ACTIONS

Three time critical recovery actions are considered in this study: recovery of operation of the PORVs, recovery of AFW flow by means of FLEX equipment, and recovery of HPI function after the room containing HPI pumps is dry. In order to support the modeling of these recovery actions, in practice it would be necessary to perform simulated recovery actions while attempting to include the additional stresses or barriers associated with an actual seismic event. For this case study, estimates were made for the probability that a recovery action could be performed within a given time period by fitting a Weibull distribution with scale factor λ and shape factor k to the probability that the equipment function would be restored by a given time as described below:

- For the recovery of AFW by use of the FLEX equipment, it was assumed that at least 1 hr was required to move the equipment from its storage location and make the necessary connections. After 1 hr, recovery is represented by a Weibull distribution with parameters $\lambda = 1.28$ and $k = 1$. The recovery probability of each system as a function of time is illustrated in Table IV. The recovery function for FLEX begins immediately after the seismic event when the failure of the AFW system is identified.
- For the recovery of HPI, it was assumed that after the water level in Room 2 in Figure 1 had receded through floor drains (See Section VII.B) that the HPI equipment could be restarted. A Weibull distribution was assumed with the values $\lambda = 1.5$ and $k = 0.85$ in obtaining Table IV HPI data. Recovery times are relative to the time T_{dry} which is the time in the accident at which Room 2 becomes dry. If Room 2 never floods, HPI may still fail on demand without recovery due to internal events.
- For recovery of PORVs, it is assumed that the electrical cabinet containing the control logic to open the PORVs has failed but that the cabinet can be accessed by operating staff within 30 minutes. Some time is then required to diagnose the problem and to obtain some means of imposing an appropriate signal to open the valves. This time period is represented by a Weibull distribution with $\lambda = 1.24$ and $k = 1.73$ in obtaining Table IV data following the first 30 minutes. However, the plant staff do not become aware that the PORVs are inoperable until the first attempt to open them remotely (T_{demand}) fails. T_{demand} equals the time at which HPI is recovered.

During the time period prior to recovery of auxiliary feed-water by means of the FLEX equipment, the primary system PORVs will cycle to relieve pressure according to their set points (Table I). Based on MELCOR analyses during the first 23 hrs the cycle rate is approximately 45 per hour and subsequently approximately 26 per hour. A stuck-open PORV failure is assessed to have the probability of 6E-3 per cycle.[9] A stuck-open PORV prior to recovery of HPI was assumed to result in core damage based on MELCOR analyses.

VII. PHENOMENOLOGICAL MODELS

The modeling of severe accident progression in MELCOR, of the transient flooding of rooms in the auxiliary building and of the magnitude and frequency of aftershocks are presented in Sections VII.A, VII.B and VII.C respectively.

VII.A MELCOR Model

The plant system is modeled in MELCOR,[7] a severe accident simulation code developed at Sandia National Laboratories for the U.S. NRC. The model is modified from a station blackout case, in which all local electrical power is eventually lost, to a loss of offsite power in which local backup power is maintained by diesel generators but the primary pumps and feedwater cannot be used. The model includes the 4-loop primary system, 4 steam generators, the containment system, and the safety systems[12]. The flow paths from the CSTs which store water for the AFW system are disabled if the CST tanks fail. If feedwater is reestablished using FLEX equipment, it is injected into the model from a source that is assumed to be inexhaustible.

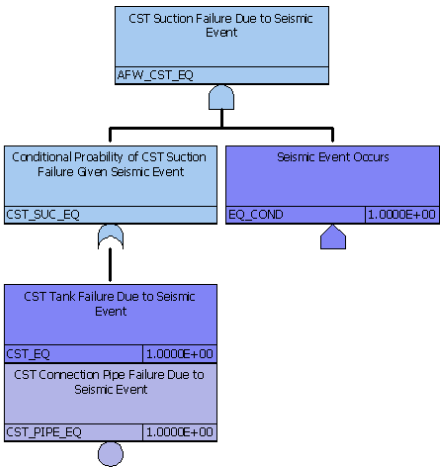

Figure 5. Subtree of CST Seismic-Induced Suction Failure

TABLE IV. Safety System Recovery Probabilities (shaded values sampled in DET)

T-T0 (hr)	FLEX T0=0	HPI T0=T_{dry}	PORV T0=T_{demand}
0	0.00	0.00	0.00
1	0.00	0.51	0.19
2	0.54	0.72	0.75
3	0.79	0.84	0.97
4	0.90	0.90	0.99
5	0.96	0.94	0.99
6	0.98	0.96	0.99
7	0.99	0.98	0.99
8	0.99	0.99	0.99

VII.B Reduced-Order Flooding Model

A Reduced-Order Flooding Model (ROFM) was developed in this project to describe the flooding of compartments following a seismic event. The model is fast running to support the performance of dynamic uncertainty analyses. The model solves differential equations for fluid flow under the assumption that a single water level characterizes the depth of water within a room. The mass balance for a compartment is merely the net sum of water flowing into and out of a room in a time step. Flow between compartments and friction in pipes are accounted for using steady state correlations. The model is highly flexible with regard to number of compartments and flow paths. The cross sectional area of a compartment can vary as a function of height to account for displacement of water by obstacles in the room such as large equipment. Configuration-dependent discharge coefficients were developed for the model by benchmarking the ROFM against results obtained with the FLUENT code[13].

VII.C After-Shock Model

A model similar to the model derived by Reasenberg[14,15] to predict the probability of aftershocks as a function of time and the magnitude of the main shock has been developed in which the size of the earthquake is measured in peak ground acceleration. The model is based on two well-known earthquake "laws", the Omori Law,[16] describing the decrease in the rate of aftershocks as a function of time after the initial earthquake and the Gutenberg-Richter[14] distribution describing the frequency distribution of aftershocks as a function of earthquake magnitude. The relationship between earthquake magnitude, Mercalli Magnitude Index (*M*), and the ground acceleration typically is described by the form of Eq. 1 in which the values of the parameters are site dependent[17].

$$M = \alpha \cdot \log(PGA) + \beta \tag{1}$$

Typical parameter values for a plant in California are α = 2.3, β = 0.92. [17] PGA is the peak ground acceleration. The mean number of shocks Λ in a given time interval is calculated from:

$$\Lambda = \int_S^T \lambda(t)dt = \left(10^a \left(\frac{PGAm}{PGA}\right)^{2.3b}\right)\left(\frac{1}{1-p}\right)\mathrm{X}\left[(T+c)^{1-p} - (S+c)^{1-p}\right] \tag{2}$$

where $\lambda(t)$ is the probability of one or more aftershocks per unit time and Λ is the mean number of aftershocks of magnitude PGA in the interval beginning with time *S* and ending with time *T* for a main shock acceleration of PGAm. The parameters *p (1.08), a (-1.67), b (0.91)* and *c* (0.05) in Eq. (2) are empirically determined characteristics of a site. The values used in this example are shown in parentheses.

There is some possibility that a shock occurring after the initial shock is larger than the initial shock. In this case the initial shock is referred to as a foreshock and the larger earthquake becomes the main shock. There is approximately a 5% probability of this occurring.[15] Because with an elastic response structures return to their initial state, if structures respond to the main shock in an elastic manner, an aftershock is unlikely to result in additional structural damage. However, an aftershock similar in magnitude to the initial shock would be uncorrelated with the initial shock and could lead to additional probability of the failure of components according to the associated fragility curve. In this case study, consideration is only given to the human response aspects of an aftershock. For the simulation of an actual event, it would be necessary to perform studies of human response to determine how the timing of response would be affected by different sizes of earthquake. For this study it was assumed that an aftershock greater than 10% of the main shock was assumed to result in a delay in completing recovery actions of 15 minutes as illustrated in Figure 6.

Figure 6. Delay Time Due to Aftershocks as a Function of Recovery Time Based on Eq.(2)

VIII. ADAPT (DYNAMIC EVENT TREE) MODEL

In order to explore different possible configurations of uncertain parameters from the flooding and aftershock models, the MELCOR plant model was run with the dynamic event tree platform ADAPT.[12] Within ADAPT and other DET codes, a simulator is run from a starting condition until a user specified time or plant conditions indicate that an uncertain event has been reached. At that point the analysis splits into as many branches as there are sampled values of the uncertain parameter and progresses in parallel.

IX. RESULTS

Section A describes the results of the flooding analysis. Section B describes the results obtained by exercising the dynamic event tree.

IX.A Flooding Analysis

In this case study the ROFM is being used to examine flooding of the two HPI rooms in the basement of the auxiliary building (see Figure 1). The timing of failure associated with the flooding of HPI pumps and the subsequent dry out of the HPI rooms is determined in the analyses for different leak rates from failed piping from the CSTs. Tables V and VI provide the volumes and flow paths in the flooding analysis. In Table V, the CST Moat in Figure 1 is a catch basin under the CSTs at the base of the CST building. The drain sump is modeled as a very large room underneath the auxiliary building to simulate an effectively infinite sink for water flowing out the floor drains in each of the rooms in the auxiliary building.

Table VII shows eight possible leak rates given the CST configuration, and provides the time of HPI failure (if any) and the time of Room 2 dryout from analyses performed for the eight leak rates using the ROFM. The Flow Area in Table VII refers to pipe-area equivalents. It may be noted that the partial failure of one pipe from each CST (Scenario 5 in Table VII) exposes the same Flow Area as the complete failure of a single pipe (Scenario 2), but causes more severe and longer-lasting flooding as both CSTs are assumed to empty through the failed pipes. Figure 7 illustrates the results for the case of a single tank failure (either tank) with a leak area associated with 2 A_p, which is Scenario 4 in Table VII. In this analysis, the water level exceeds 0.67m at 385 seconds into the scenario, which would result in failure of the charging pump. At 1,275 seconds the door between the two basement rooms fails and the HPI pumps soon fail. At 4,840 seconds, the water level is effectively zero and actions could be taken to attempt to restart the safety injection pumps. In order to reduce the scope of the DET analysis, only three flooding scenarios were included in the analysis: Flooding Scenarios 4, 5 and 7 in Table VII. Effectively, Scenario 4 represents all scenarios involving the seismic failure of one tank. Because Scenarios 1 and 2 don't lead to HPI failure, this

approximation is expected to over-estimate core damage frequency. Scenario 5 represents Scenarios 5 and 6 and Scenario 7 represents Scenarios 7 and 8.

TABLE V. Compartment Information

Room	Name	Area (m^2)	Max. Elev. (m)	Min. Elev. (m)
1	Auxiliary CST	45.6	6.23	0
2	Main CST	45.6	6.23	0
3	CST Moat	167.23	1.524	0
4	Auxiliary Building	278.71	4	0
5	Auxiliary Basement Room 1	13 9.36	0	-4
6	Auxiliary Basement Room 2	139.36	0	-4
7	Sump	278.71	-4	-10

TABLE VI. Flow Path Information

Path	From Room / To Room	Area (m^2)	Dia-meter (m)	Length (m)	From/To Elevation (m)
1	1/3	0.03	0.2	1	0/0
2	1/3	0.03	0.2	1	0/0
3	2/3	0.03	0.2	1	0/0
4	2/3	0.03	0.2	1	0/0
5	3/4	1	0.5	1.5	0/0
6	4/5	6	2.4	1	0/0
7	5/6	2.2	1.4	0.1	-3.3/-3.3
8	5/7	0.005	0.08	1.5	-4/-4
9	6/7	0.005	0.08	1.5	-4/-4

TABLE VII. Results of Flow Analyses (shaded values sampled in DET)

Flooding Scenario Number	CST Failure	Flow Area (A_p)	Time of HPI Failure (s)	Time of Dryout (s)
1	One	0.5	N/A	N/A
2	One	1	N/A	N/A
3	One	1.5	2295	5285
4	One	2	1310	4840
5	Two	1	2335	9410
6	Two	2	985	8710
7	Two	3	640	8475
8	Two	4	470	8545

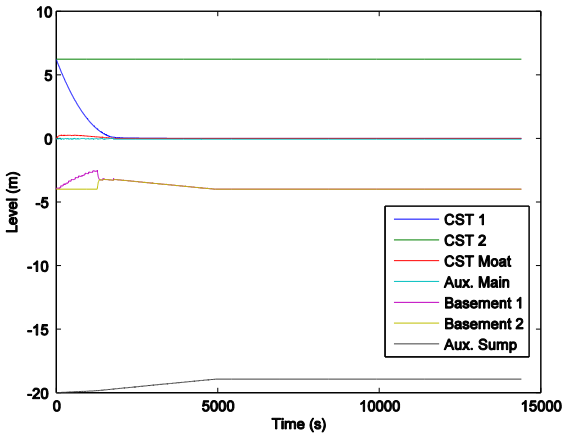

Figure 7. Water Levels in Flood Analysis

IX.B DET Analysis

In this section, the DET analysis is described including the common cause effects of flooding on system failure. Results are presented for the quantification of core damage frequency and importance of recovery events. In this example, the only internal events included in the analysis were the random failure of the HPI pumps and the random failure of one pathway for feed-water for Scenario 4 in which only one of the CSTs is failed. The dynamic analysis of Scenarios 4, 5, and 7 (see Table VII, shaded portions) associated with different flooding rates was performed.

Four samples each were taken from the distributions for AFW and HPI recovery time (see Table IV, shaded portions), and 3 samples were taken for recovery of PORV control after recovery of HPI pumps. The simulation is stopped at 1, 2, 3, and 4 hours to assess the impact of aftershocks. At each stopping point, an aftershock may occur, adding 15 minutes to all recovery actions. This time is representative of the time lost as plant personnel take shelter during an aftershock.

In all, 14 branching conditions were applied in the dynamic analysis, resulting in 6,316 unique sequences. Three flooding scenarios were selected to span the range of potential HPI room dryout times. The DET analysis is performed conditional on pre-existing state of the plant, e.g. whether one of the redundant pathways for AFW flow was in a failed state due to a random

fault (internal event fault) in addition to the loss of AFW pathway(s) due to flooding resulting from the specific flooding scenario being analyzed. Thus, the analysis for each flooding scenario begins assuming a probability of 1, and applies the conditional probability of each value of each branching condition to determine the total probability of each sequence conditional on the incoming plant state. In this way, the probability of fuel damage is calculated for each flooding scenario.

One of the positive features of DET analyses is the consistent approach to the identification of possible scenarios. By identifying the characteristics of scenarios that either lead to core damage or avoid core damage, insights can be obtained regarding preferred accident management strategies.

Tables VIII, IX, and X examine the fraction of DET scenarios resulting in core damage by timing of AFW recovery, flooding scenario, and timing of HPI recovery after flooding recedes, respectively. These represent three different ways of parsing the same results for core damage probability. Fuel damage is marked by any release of fission products from fuel pins. The earlier that AFW is recovered, the higher the likelihood of recovery without core damage. The maximum core damage fraction of 2.0E-3 occurs for AFW recovery range of 0-3 hours (see Table VIII). The maximum occurs early in time because the likelihood of successful implementation of the FLEX equipment by 3 hours was assessed to be quite high (see Table IV). For AFW recovery at 3.5 hr, the probability of core damage was assessed to have risen to 70%. For AFW recovery later than 4 hours, the likelihood of fuel damage was found to be nearly 100% but very few scenarios have recovery times this late.

For Scenario 4, only one CST fails as the result of seismic load. The other train of AFW can be lost as the result of random failure (based on the plant's internal events PRA, with a failure on demand probability of 1.2E-3) but the combined probability leading to the loss of AFW is small. However, core damage is also possible without loss of AFW due to flooding and failure to recover HPI and PORV operability. Once PORVs and HPI are recovered, it is assumed the PORVs will be opened to reduce primary pressure. When the operating range for HPI (see Table I) is reached, makeup is provided for the primary inventory being vented through the PORVs. The operating range of the LPI system (see Table I) can then be reached, allowing the delivery of a large amount of cooling water to the primary system. If this state is reached without fuel damage, the scenario is assumed to end in success. In Scenario 4 loss of HPI occurs early. However, in comparison with Scenarios 5 and 7, room dryout with the potential for recovery of HPI and PORV operability occurs much earlier in time. Because Scenario 4 has a higher probability and the operator initiates feed and bleed earlier in the scenario at a time in which decay heat level is higher, the probability of core damage is higher for Scenario 4 than for Scenarios 5 and 7. For this plant design, if AFW is not lost or is recovered early, a preferred severe accident management strategy might be to delay the initiation of feed and bleed until the probability of successful depressurization without core damage is higher.

TABLE VIII. Core Damage Fraction by AFW Recovery Time Range

AFW Recovery Range	Probability
0 to 3 hours	2.0E-3
3 to 3.5 hours	1.2E-5
3.5 hours and up	7.5E-6

TABLE IX. Core Damage Fraction by Flooding Scenario (see Table VII)

Sequence	Probability
Flooding Scenario 4	1.2E-3
Flooding Scenario 5	4.0E-4
Flooding Scenario 7	2.3E-4
No Flooding	1.8E-11

TABLE X. Core Damage Fraction by HPI Recovery Time after Dryout

Sequence	Probability
0 to 2 hours	1.1E-5
2 to 3 hours	1.3E-3
3 to 4 hours	6.4E-4
4 hours and up	5.1E-5

X. CONCLUSIONS

The process of defining and running a DET analysis of a seismic event at a PWR was demonstrated. The expected range of the severity of CST pipe damage was assessed using structural analysis of the pipes subject to seismic loads, and the extent of the ensuing flood was estimated using a reduced-order room flooding model. Probabilistic models were developed for the likelihood of successful recovery of systems as a function of time. Using samples from the various assumed probability distributions to define scenarios, a DET analysis was performed in which the MELCOR computer code was used to determine which scenarios would or would not lead to core damage. The likelihood of aftershocks and direct seismic damage were also

considered in the DET analysis. The DET analysis yielded insights into the impact of multiple pipe and tank failures on plant flooding, as well as the impact of the recovery of normal operation of key safety systems.

Although historically little credit has been given in PRAs to recovery actions, the Fukushima accident has shown the potential importance of operator response and recovery actions to the mitigation of accident consequences. The performance of a complete SPRA using DET methodology would be expensive. This study indicates how DETs can be used effectively in examining circumstances in which timing of response actions is important.

ACKNOWLEDGEMENT

This research is being performed using funding received from the DOE Office of Nuclear Energy's Nuclear Energy University Programs. The support provided for the project NEUP 13-5132 is greatly acknowledged.

REFERENCES

1. H. SEZEN, J. HUR, M. KOSE, R. DENNING, and T. ALDEMIR, "Mechanistic and Probabilistic Seismic Assessment of Structures and Components in Nuclear Power Plants" *SMIRT-23 Conference (Structural Mechanics in Reactor Technology)*, Manchester, United Kingdom, (2015).
2. D. GASTON, G. HANSEN and C. NEWMAN, "MOOSE: A Parallel Computational Framework for Coupled Systems of Nonlinear Equations," *INL/CON-08-15008*, Idaho National Laboratory, Idaho Falls, ID, (2009)
3. A. ALFONSI, C. RABITI, D. MANDELLI, J. COGLIATI, and R. KINOSHITA, "RAVEN as a Tool for Dynamic Probabilistic Risk Assessment: Software Overview," *International Conference on Mathematics and Computational Methods Applied to Nuclear Science & Engineering*, (M&C 2013), (2013).
4. Nuclear Energy Institute, "Diverse and Flexible Coping Strategies (FLEX), Implementation Guide," *NEI 12-06*, Washington, D.C. (2012)
5. T. ALDEMIR, "A Survey of Dynamic Methodologies for Probabilistic Safety Assessment of Nuclear Power Plants," *Annals of Nuclear Energy*, **52**, 113-124 (2013)
6. A. GULER, J. HUR, Z. JANKOVSKY, H. SEZEN, T. ALDEMIR and R. DENNING, "A Dynamic Treatment of Common Cause Failure in Seismic Events," *Proceedings of the 2016 International Congress on Advances in Nuclear Power Plants*, San Francisco, CA, (2016).
7. Sandia National Laboratories, "MELCOR Computer Code Manuals, Vol. 2: Reference Manuals," Version 1.8.6, *NUREG/CR-6119*, (2006).
8. M. K. RAVINDRA, "Session III. SPRA Methodology Seismic Fragility Analysis," *Proceeding of Post-Symposium Seminar: Seismic PRA: Post-Fukushima Implementation*, North Carolina, (2014).
9. K. METZROTH, "A Comparison of Dynamic and Classical Event Tree Analysis for Nuclear Power Plant Probabilistic Safety/Risk Assessment," Dissertation, The Ohio State University, (2011).
10 US NRC, "Severe Accident Risks: An Assessment for Five U.S. Nuclear Power Plants," NUREG-1150, Washington, DC, December 1990.
11. US NRC, "Risk Assessment of Operational Events-Handbook", Volume 2, External Events, Rev. 1.01, 2008.
12. U. CATALYUREK, B. RUTT, K. METZROTH, A. HAKOBYAN, T. ALDEMIR, S. DUNAGAN, D. KUNZMAN, "Development of a Code Agnostic Computational Infrastructure for the Dynamic Generation of Accident Progression Event Trees," *Reliability Engineering and System Safety*, **95**, pp.278-294, (2010).
13. ANSYS, "ANSYS/FLUENT 12.0 User's Guide," www.ansys.com, (2009).
14. P. A. REASENBERG and L. M. JONES, "Earthquake Hazard After a Mainshock in California," *Science*, **243**, pp 1173-1176, (1989).
15. P. A. REASENBERG and L. M. JONES, "Earthquake Aftershocks: Update," *Science*, **265**, pp 1251-1252, (1994).
16. T. UTSU, Y. OGATA and R. S. MATSURA, "The Centenary of the Omori Formula for a Decay Law of Aftershock Activity," *J. Phys. Earth*, **43**, pp1-33, (1995).
17. L. LINKIMER, "Relationship Between Peak Ground Acceleration and Modified Mercalli Intensity in Costa Rica," *Revista Geologica de America Central*, **38**, pp. 81-94, (2008).